Costoclavicular Compression of the Brachial Plexus in a Patient With a Right Aortic Arch: MRI/MRA/MRV

James D. Collins, MD

Keywords: radiology ■ imaging ■ anatomy ■ costoclavicular compression ■ Batson's plexus ■ magnetic resonance imaging ■ magnetic resonance angiography ■ magnetic resonance venography ■ aorta

J Natl Med Assoc. 2012;104:567-575

Author Affiliations: University of California at Los Angeles, Department of Radiological Sciences, Los Angeles, California.
Correspondence: James D. Collins, MD, University of California at Los Angeles, Department of Radiological Sciences, 10833 Le Conte Ave, BL-428 CHS/UCLA mail code 172115, Los Angeles, CA 90095 (jamesc@mednet.ucla.edu).

INTRODUCTION

The circulatory system is a closed system. Any decrease in venous return increases intrathoracic, intraabdominal, and intracranial pressures. This fact may be simply observed by application of an inflated blood pressure cuff, tourniquet, or hands around a patient's upper arm visually dilating the superficial veins of the forearm.[1] The venous drainage marginated by lymphatics is diverted into the deeper fascial planes of the arm. The patient experiences the sensation of throbbing-like increased pressure from expansion of the deeper fascial planes reciprocally increasing arterial pressure.[2] Bicuspid valves present within peripheral veins and lymphatics along their course proximal to junctions with other veins and lymphatics assist, direct, and divert venous and lymphatic flow into other veins and lymphatics.[3] Since nutrient arteries, veins, and lymphatics within fascial planes supply nerves and other structures throughout the human body,[4] costoclavicular compression of the brachial plexus nerves compromises nutrient arterial supply and dilates veins and lymphatics, diminishing return to the heart. The resulting dilatation of the veins and lymphatics expands fascial planes (edema). Ischemia develops, and if not relieved, tissue damage follows.[1]

Two patients from our database with the clinical diagnosis of thoracic outlet syndrome (TOS) presented with severe hoarseness and dysphagia.[5-8] Both cases displayed right aortic arch and left aberrant subclavian artery with posterior displacement of the ascending aorta and posterior anterior compression of the esophagus against the trachea. Both patients underwent bilateral magnetic resonance imaging (MRI), magnetic resonance angiography (MRA), and magnetic resonance venography (MRV) of the brachial plexus to determine the sites of compression because the clinicians were aware of our procedure. Both patients were diagnosed with costoclavicular compression of the arterial flow to the brachial plexus nerves and compression of the veins and lymphatic draining the brachial plexus. One patient was selected because she had ruptured her saline breast implants. They were replaced by silicone implants, which caused fibrosis and scarring over the anterior chest wall muscles and limited motion of her upper extremities. Since it is not possible to present all of the images acquired, those selected best demonstrate the anatomy and pathophysiology.

CLINICAL HISTORY

This is a 51-year-old right-handed female who presented to her neurologist with bilateral throbbing-like frontal temporal headaches that radiated from the back of the head into her eyes. At night, headaches would often awaken her. The headaches were described as 10 out of 10 in terms of pain and occurred 1 to 2 times a month without any triggered known causes. Stress aggravated her headaches. She also had associated symptoms of nausea, vomiting, photophobia, phonophobia, and osmophobia.

Physical Examination

Findings from her physical exam include: height, 1.6 m; weight, 58.5 kg; temperature, 36.8ºC; blood pressure, 115/68 mm Hg; pulse, 74 beats/min; and respiratory rate, 17 breaths/min. A review of systems pertaining to her headaches included: frank motor weakness, dysphasia, incoordination, sensory changes, low-grade tinnitus in the left ear that lasted sometimes for 3 weeks with associated diplopia, sometimes hearing loss dysarthria and vertigo. Her only medication was topiramate, 100 mg 4 times daily.

Her medical history included a long time of difficulty in swallowing (dysphagia), particularly stewed meals; bilateral saline breast implantations for augmentation, which ruptured; breast implants replaced with silicone, which decreased her upper-extremity range of motion; right elbow tendonitis for which she underwent ulnar nerve transposition and had recently repaired (approximately 2 months prior to her initial evaluation); and ongoing physical therapy designed for TOS patients.

Because the clinical diagnosis of TOS was suspected, bilateral MRI, MRA, and MRV of the brachial plexus were requested to detect the sites of brachial plexus compression.

METHODS AND MATERIALS

Plain chest radiographs (posterior-anterior and lateral) were obtained and reviewed prior to the MRI. The procedure was discussed and the patient examined. Respiratory gating was applied throughout the procedure to minimize motion artifact. The patient was positioned supine in the body coil, arms down to the side, and imaging was monitored at the MRI station. Magnetic resonance images were obtained on the 1.5-Tesla GE Signa MR scanner (GE Medical Systems, Milwaukee, Wisconsin). A body coil was used and intravenous contrast agents were not administered. A saline water bag was placed on the right and the left side of the neck to increase signal to noise ratio for high-resolution imaging. A full field of view (44 cm) of the neck and the thorax was used to image both supraclavicular fossae. Contiguous (4 mm) coronal, transverse (axial), transverse oblique, sagittal, and abduction external rotation (AER) of the upper extremities coronal T1-weighted and 2-dimensional time-of-flight MRA and MRV images were obtained. Where there was clinical evidence of scarring, tumor, and/or lymphatic obstruction, fast-spin echo T2-weighted images were selectively obtained. The parameters for acquiring each sequence have been published.[1]

Figure 1. Posterior-anterior view of the right aortic arch (A) descending right of midline compressing the trachea (T) anterior laterally left

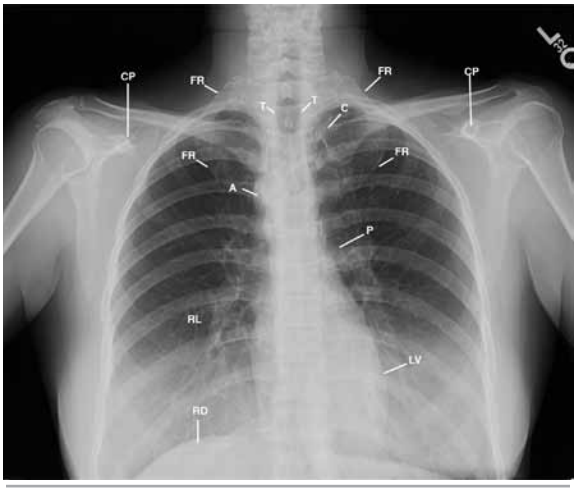

C indicates clavicle; CP, coracoid process; FR, first rib; LV, left ventricle; P, pulmonary artery; RD, right diaphragm.

DIAGNOSTIC STUDIES

Posterior-anterior and lateral chest radiographs with anterior-posterior cervicothoracic spine were obtained. No previous chest films were available for comparison.

Findings

The posterior-anterior chest radiograph (Figure 1) displays mild erosion of the uncovertebral joints at the level of C4-5, right greater than left; incomplete ossification of the right transverse process of the first thoracic vertebra; small calcification over the region of the supraspinatus tendon marginating the head of the left humerus; right aortic arch descending off right of midline, displacing the trachea anterior laterally left; straight right pericardium, reflecting old inflammatory disease; bilateral hazy breast implantations; anterior-rotated heads of the clavicle over the posterior third intercostal spaces, right lower than left; drooping of the right shoulder as compared to the elevated left, and the mildly dilated right

Figure 2. Anterior bowed body of the sternum (S); backward-displaced manubrium (M): concave posterior margin of the trachea (T) secondary to the bulbous expanded right aortic arch, and bilateral round shoulders (X)

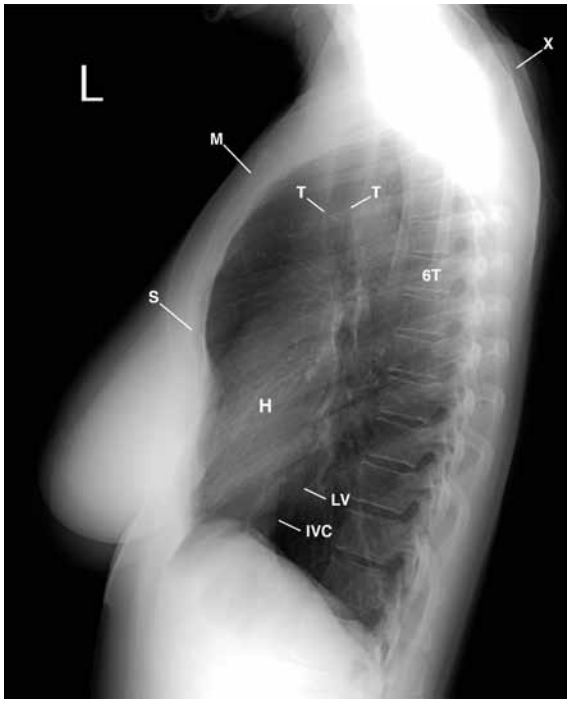

6T, sixth thoracic vertebra; H indicates heart; IVC, inferior vena cava; L, left-sided lateral chest; LV, left ventricle.

main stem bronchus, otherwise normal lungs.

The lateral chest radiograph (Figure 2) cross-references the posterior-anterior chest radiograph to display the anterior bowed body of the sternum; backward-displaced manubrium: concave posterior margin of the trachea secondary to the bulbous expanded right aortic arch; bilateral rounding of the shoulders; silicone breast implants as per history given; and normal lungs.

The anterior-posterior cervicothoracic spine radiograph (not displayed) cross-referenced the findings above to display degenerative changes involving the uncovertebral joints at the level of C4-5, right greater than left, and the right aortic arch displacing the trachea anterior laterally at the 3T-4T vertebrae.

Conclusion

Right aortic arch is as described above. Additionally, we found: anterior bowed body of the sternum displacing the manubrium posteriorly; degenerative changes as above C4-5; bilateral silicone breast implants as per history given; and bilateral round shoulders, right greater than left.

FINDINGS FROM MAGNETIC RESONANCE IMAGING

The multiplanar MRI captured images that displayed the right aortic arch; aberrant left subclavian artery taking origin from the bulbous dilated aorta (diverticulum of Kommerell) ascending posterior-lateral to the dilated esophagus; posterior-anterior compressed esophagus

Figure 3. Right aortic arch (A) and aberrant left subclavian artery (AB L SA) taking origin from the bulbous dilated aorta (diverticulum of Kommerell)

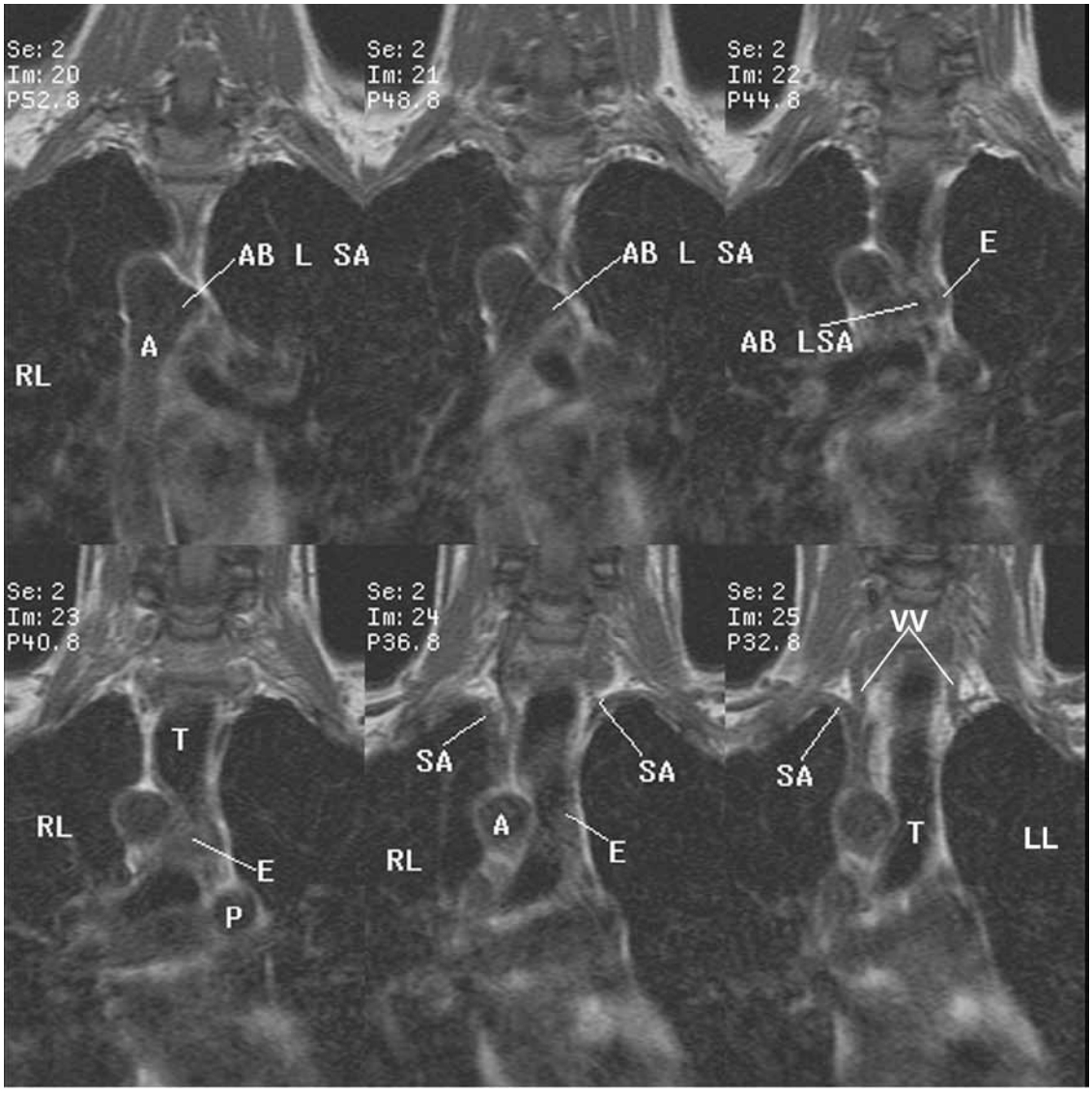

E indicates esophagus; LL, left lung; P, pulmonary artery; RL, right lung; SA, subclavian artery; T, trachea; VV, vertebral veins.

and trachea to the left of midline and the dilated anterior vertebral veins, right greater than left, reflecting impedance to venous return (Figure 3); right and left common carotid arteries originating from the aorta; bilateral asymmetric costoclavicular compression of the subclavian and axillary veins, right greater than left; impedance to venous return within the left brachiocephalic vein (Figure 4); aberrant ascending left subclavian artery; superior sternopericardial ligament attaching the cardiomediastinal structures to the manubrium off right of midline; dilated azygos vein, and the retro esophageal descending aorta compressing the esophagus against the trachea, which explains her long history of dysphagia (Figure 5); diverticulum of the aorta compressing the esophagus against the trachea, clavicle with the backward manubrium compressing the left brachiocephalic vein against the ascending arch of the aorta; compressed inferior bicuspid valve within the right internal jugular vein against the dilated anterior right vertebral vein and the course of the azygos vein into the region of the superior vena cava (Figure 6); right hepatic cyst displayed on the coronal fast-spin echo sequence (not displayed); dilated vertebral venous plexus marginating the spinal cord; dilated anterior vertebral vein, right greater than left; dilated high proton-dense left brachiocephalic vein, dilated valveless right anterior jugular vein; bilateral common carotid arteries exiting the aorta; medial compressed region of the right internal jugular and brachiocephalic veins; bilateral compressed subclavian arteries at the site of binding nerve roots; bilateral occipital veins draining into the asymmetric external jugular veins; ascending origin of the aberrant left subclavian

Figure 4. Images anterior to Figure 3, displaying the bulbous dilated gray proton-dense right subclavian vein (SV) on the low right first rib with the dilated gray proton-dense right axillary vein (AXV)

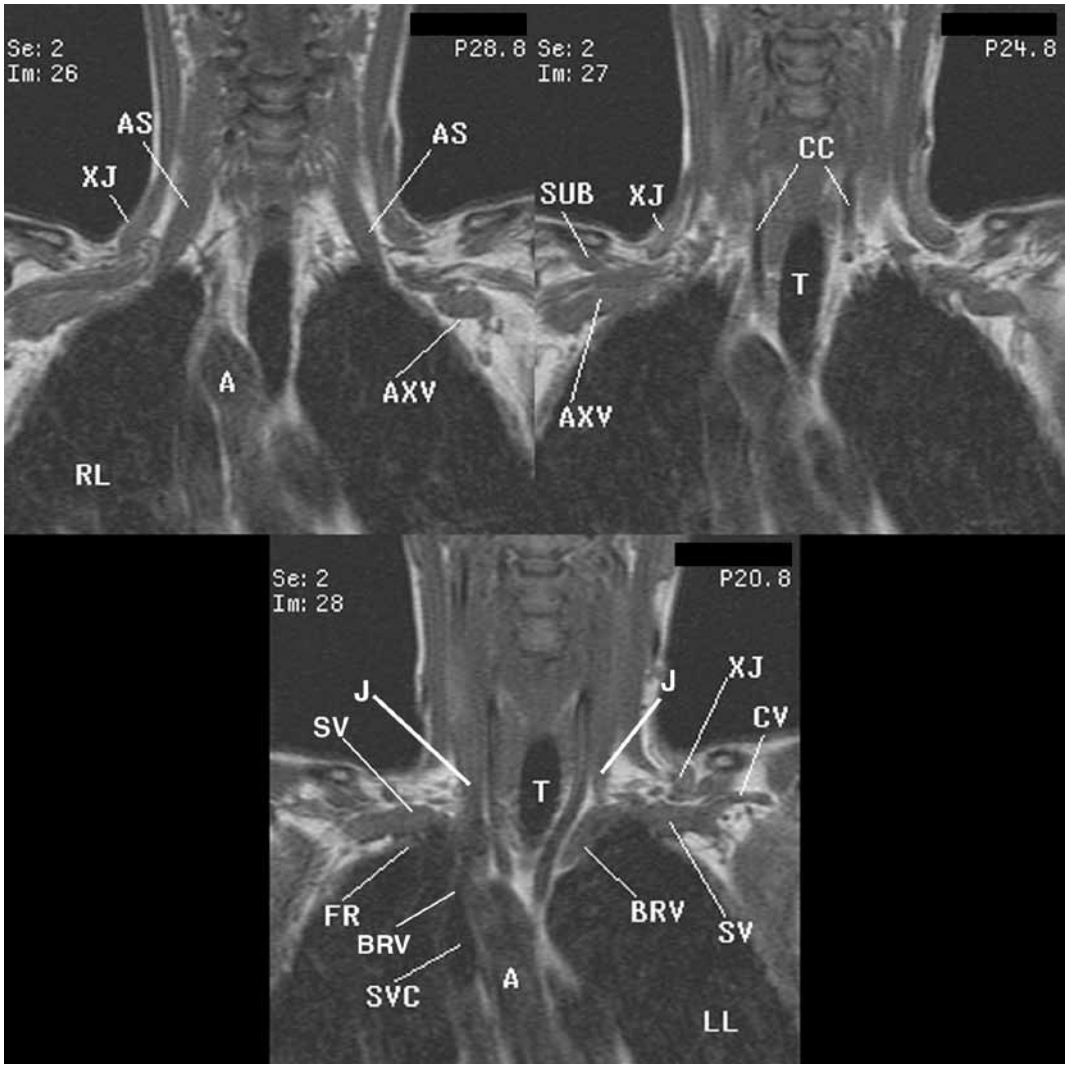

A indicates aorta; AS, anterior scalene muscle; BRV, brachiocephalic vein; CC, common carotid arteries; CV, cephalic vein; FR, first rib; J, jugular vein; LL, left lung; RL, right lung; SUB, subclavius muscle; SV, subclavian vein; SVC, superior vena cava; T, trachea; XJ, external jugular vein.

artery from the aortic diverticulum of Kommerell; and the asymmetric costoclavicular compression of the axillary arteries and veins (Figure 7); gray proton-dense asymmetric silicone breast implants adherent to the pectoralis major; and serratus anterior muscles on the arms overhead maneuver (AER) (Figure 8).

Conclusion

Our final findings included: postrupture saline breast implants replaced with silicone as described above; postrepair ulnar release right elbow with ongoing physical therapy; right aortic arch as described above; aberrant left subclavian artery; intact silicone breast implants; posterior-anterior compressed esophagus against the trachea by the bulbous expanded right-sided aorta as it gives origin to aberrant left subclavian artery; bilateral costoclavicular compression (laxity of the sling/erector muscles-trapezius, levator scapulae, serratus anterior) of the bicuspid valves within the draining veins of the neck, supraclavicular fossae with lymphatics with compression

Figure 5. Images 3, 5, 6, 10, 11, and 15 from the transverse sequence displaying the ascending aberrant left subclavian artery (SA); superior sternopericardial ligament (not labeled) attaching the cardiomediastinal structures off right of midline to the manubrium (M), dilated azygos vein (AZ) as it drains into the superior vena cava (SVC); diverticulum of the descending aorta compressing the esophagus (E) backward against the trachea (T) left of midline; backward manubrium with the clavicle (C) compressing the left brachiocephalic vein (not labeled) against the ascending aorta and the right common carotid artery (CC)

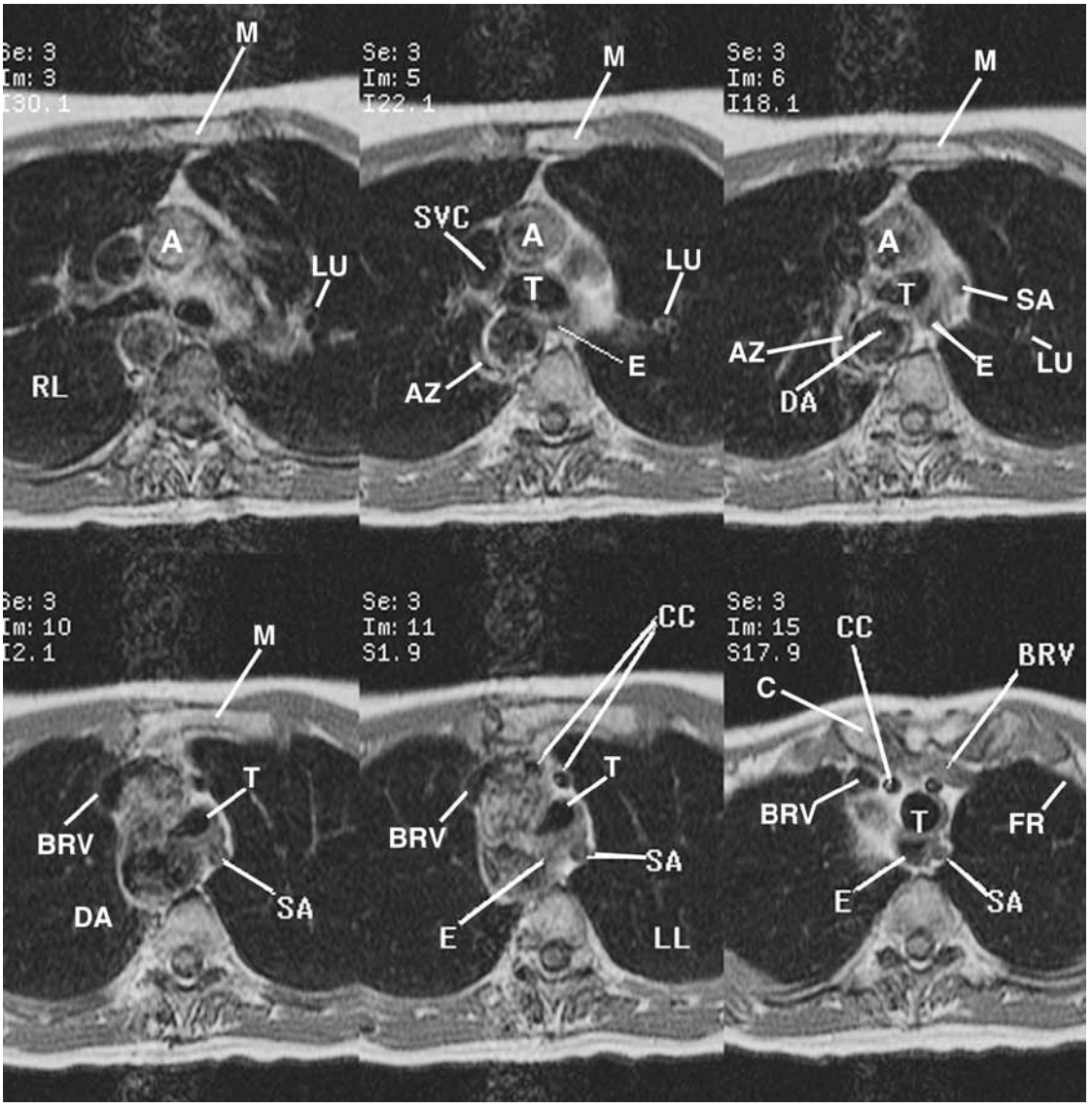

A indicates aorta; DA, descending aorta; FR, first rib; LU, left upper lung bronchus; RL, right lung.

of the subclavian and axillary arteries as above described; bilateral AER of the upper extremities, which had triggered complaints as above described; dysphagia secondary to a right-sided aorta that compressed the anteriorly displaced compressed esophagus against the trachea as described above.

DISCUSSION

A right aortic arch arises from interruption of the aortic arch between the left common carotid and the left subclavian arteries. The aorta descends on the right. The left aberrant subclavian artery courses posterior to the trachea and esophagus as in this patient. The posterior-anterior and lateral chest radiographs confirmed the unsuspected presence of the right aortic arch with compression of the posterior margin of the trachea by the diverticulum of the descending aorta prior to the bilateral MRI, MRA, and MRV imaging of the brachial plexus; bilateral hazy breast implants; anterior-rotated heads of the clavicles over the posterior third intercostal spaces, right lower than left; drooping of the right shoulder as compared to the elevated left; anterior bowed body of the sternum with the backward displaced manubrium; and bilateral rounding of the shoulders. Bilateral rounding of the shoulders increased the asymmetric slopes of the first ribs, backwardly displacing the manubrium with the clavicles and sternocleidomastoid muscles that compressed the aorta, left brachiocephalic vein

Figure 6. Sagittal images 38 through 43 at the diverticulum of Kommerell (D) displacing the gray proton-dense esophagus (E) anteriorly against the trachea (T) against the aorta (A), backward manubrium (M) with clavicle (C) compressing the left brachiocephalic vein (BRV) against the ascending arch of the aorta (A), costoclavicular compression of the region of the inferior bicuspid valve within the right internal jugular vein (J) obstructing the dilated right anterior vertebral vein (VV)

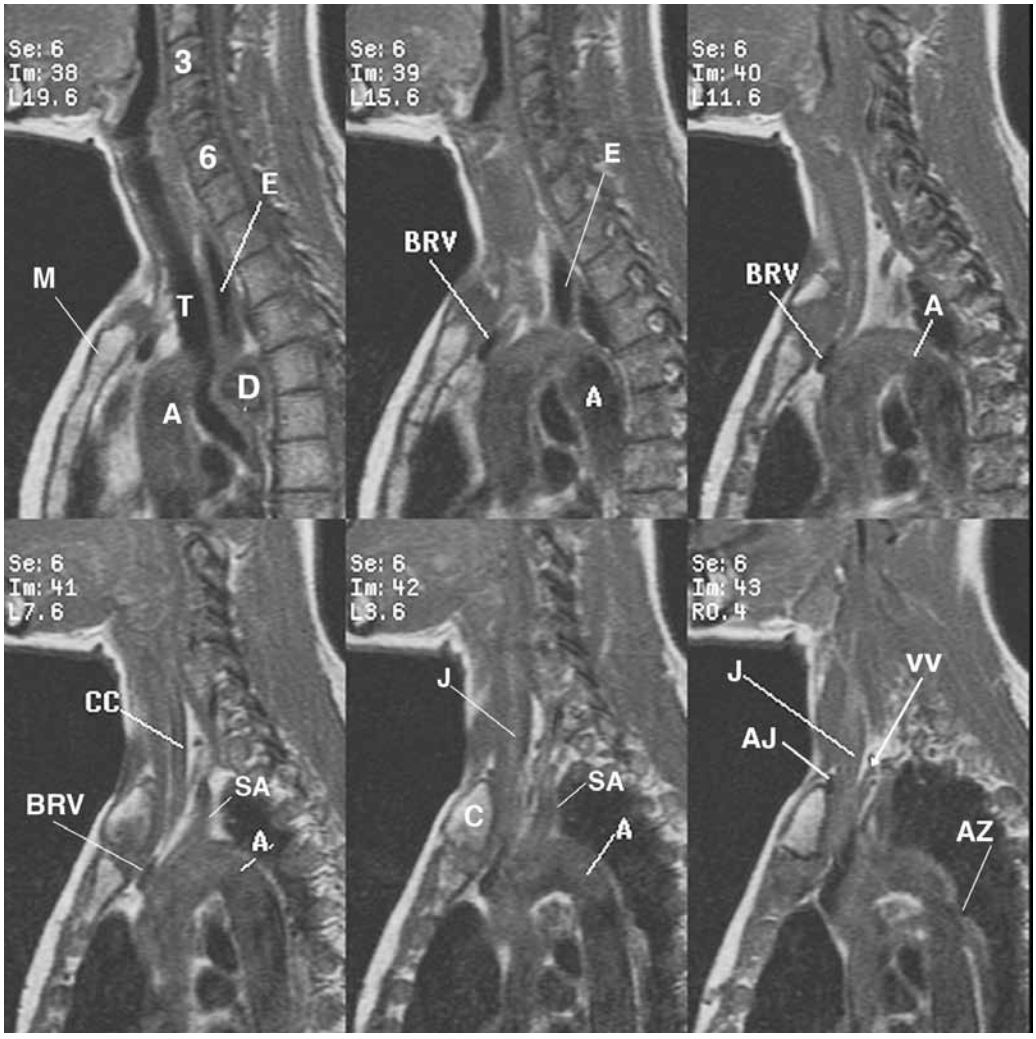

Observe the course of the azygos vein (AZ) advancing into the region of the superior vena cava (not labeled) and the right subclavian artery (SA) ascending into the region of the right scalene triangle (not labeled), 3 and 6 indicate cervical vertebrae CC, right common carotid artery; .

against the internal jugular veins medially at the inferior bicuspid valves, right greater than left.

Bilateral costoclavicular compression (laxity of the sling/erector muscles—trapezius, levator scapulae, serratus anterior) of the bicuspid valves within the draining veins of the neck and supraclavicular fossae with lymphatics compressed the subclavian and axillary arteries with binding nerves, right greater left.[3] The T1-weighted coronal and sagittal images captured the aortic diverticulum compression of the esophagus and trachea, as above described, that reflected difficulty in swallowing; costoclavicular compression of the bicuspid valves within the subclavian and external jugular veins diverting venous return within the neck into the asymmetric compressed brachiocephalic veins; compression of the inferior bicuspid valve within the right internal jugular vein against the right anterior vertebral vein as it drained into the right brachiocephalic vein backwardly dilating the vertebral venous/Batson's plexus return marginating the spinal cord.[9-12] Mild fibrosis was displayed, marginating the right scalene triangle. The stacked and 3-dimensional, reconstructed MRA and MRV images confirmed the aforementioned findings, including the course of the aberrant left subclavian artery compressed in the scalene triangle, costoclavicular compression of the second division of the right subclavian artery, and compression of the second division of aberrant left subclavian artery. The coronal fast-spin echo sequence confirmed the above findings, including the high proton-dense lymphatics, marginating veins and the hepatic cyst. AER of the upper extremities, captured by images, triggered complaints of an uncomfortable sensation over the right shoulder and a tired-like sensation over the left shoulder.

Basically, this patient developed bilateral costoclavicular compression (laxity of the sling/erector muscles-trapezius, levator scapulae, serratus anterior) of the bicuspid valves within the draining veins of the neck, supraclavicular fossae with lymphatics with compression of the subclavian and axillary arteries as described above. Bilateral coronal AER of the upper extremities enhanced costoclavicular compression in the supine position and displayed functional anatomic imaging that triggered complaints. However, the patient had taken an unknown quantity of acetaminophen pills prior to monitored imaging, which may have diminished the severity of the triggered complaints registered. She had no back, leg, or eye concerns, but she was dizzy and lightheaded upon completion of the procedure. After requesting her to cough a few times, the dizzy sensation and lightheaded sensation resolved.

Figure 7. Images 2 and 11 out of 150 from the 3-dimensional reconstructed images of the 2-dimensional time of flight MRA and MRV of the brachial plexus

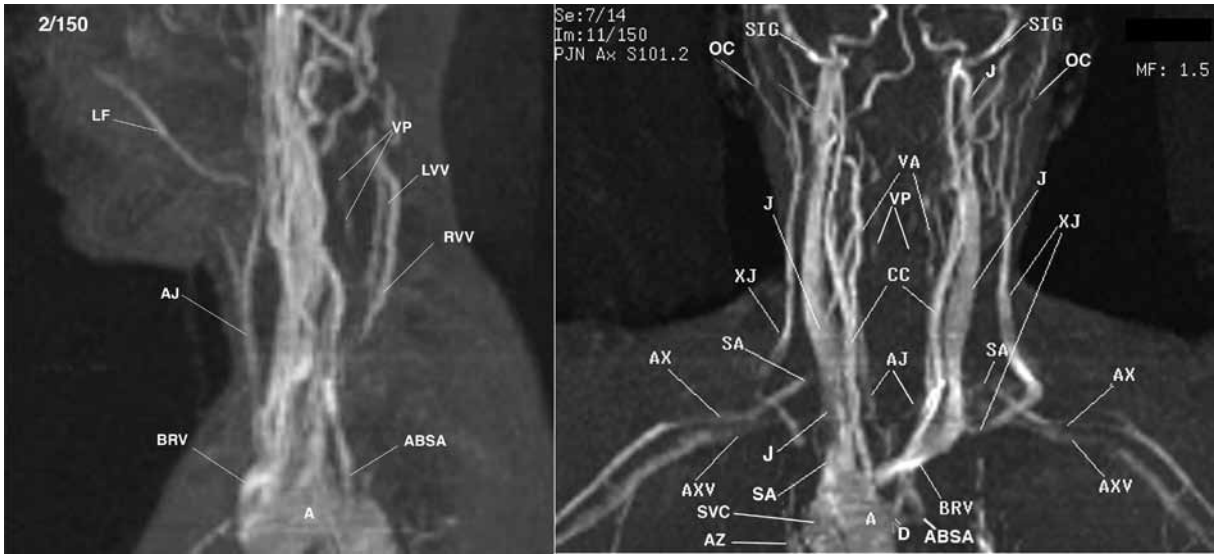

Image 2/150 displays the high proton-dense left facial vein (LF) draining into the left external jugular vein (not labeled); high dense valveless anterior jugular vein (AJ) diverting venous return back into the neck, right posterior to the left (not labeled); high proton-dense left brachiocephalic vein (BRV) reflecting impedance to venous return from the backward compression of the manubrium (not displayed); aberrant left subclavian artery (ABSA) ascending from the region of the diverticulum of Kommerell (D). Observe the high proton-dense vertebral venous / Batson's plexus (VP) marginating the region of the spinal cord anterior to the left vertebral (vein LVV) and right vertebral (RVV) vein, left higher proton-dense than the right vertebral vein.

Image 11/150 displays the dilated vertebral venous plexus (VP) marginating the region of the spinal cord; dilated high proton-dense left brachiocephalic vein (BRV) reflecting impedance to venous return as above described; dilated valveless right anterior jugular vein (AJ) greater than left; bilateral common carotid arteries (CC) exiting the aorta (A), medial compressed region of the right internal jugular vein (J) and brachiocephalic veins (BRV), bilateral compressed subclavian arteries (SA) at the site of binding nerve roots, bilateral occipital veins (OC) draining into the asymmetric external jugular veins (XJ); ascending origin of the aberrant left subclavian artery (ABSA) from the aortic diverticulum (D), and the asymmetric costoclavicular compression of the axillary arteries (AX) and axillary veins (AXV).

AZ indicates azygos vein; SVC, superior vena cava; VA, vertebral arteries; SIG, sigmoid sinus.

TAKE-HOME MESSAGE

Knowledge of normal surface and landmark anatomy is important for interpretation of MRI, MRA, and MRV studies in patients with brachial plexopathy. Since the circulatory system is a closed system, any decrease in venous return increases intrathoracic, intra-abdominal, and intracranial pressures. Veins proximal to sites of obstruction accompanied by lymphatics dilate diverting venous and lymphatic flow into collaterals, as in our patient, with obstruction to the brachiocephalic veins.[13] The valveless anterior jugular vein and occipital veins displayed emissary venous drainage releasing pressure from within the cranial vault. The obstruction of the right anterior vertebral vein dilated the vertebral venous plexus, marginating the spinal cord, as displayed on the 2-dimensional time-of-flight MRA and MRV. The reader should recall that the vertebral venous plexus/Batson's plexus drainage of the spinal canal has a large, valveless network of vertebral veins that have glistening lymphatics when imaging fresh tissue and embalmed cadavers by flash-assisted lighting.[11] Any decrease in venous return in vivo also dilates the vertebral venous plexus of the spinal canal as part of the circulatory system. The clinical presenting symptoms of TOS and dysphagia should indicate to radiologists and other health professionals that costoclavicular compression of the brachial plexus should be suspected and detected by monitored imaging with bilateral MRI, MRA, and MRV of the brachial plexus. In addition, the detection of the unsuspected right aortic arch on the chest radiographs should

Figure 8. Coronal image 31 of 33 from the abduction external rotation sequence of the arms overhead maneuver to demonstrate the adhesions (scarring) of the gray proton-dense silicone breast implants (B) to the anterior chest against the pectoralis major muscles (PM) and the serratus anterior muscle (SAM)

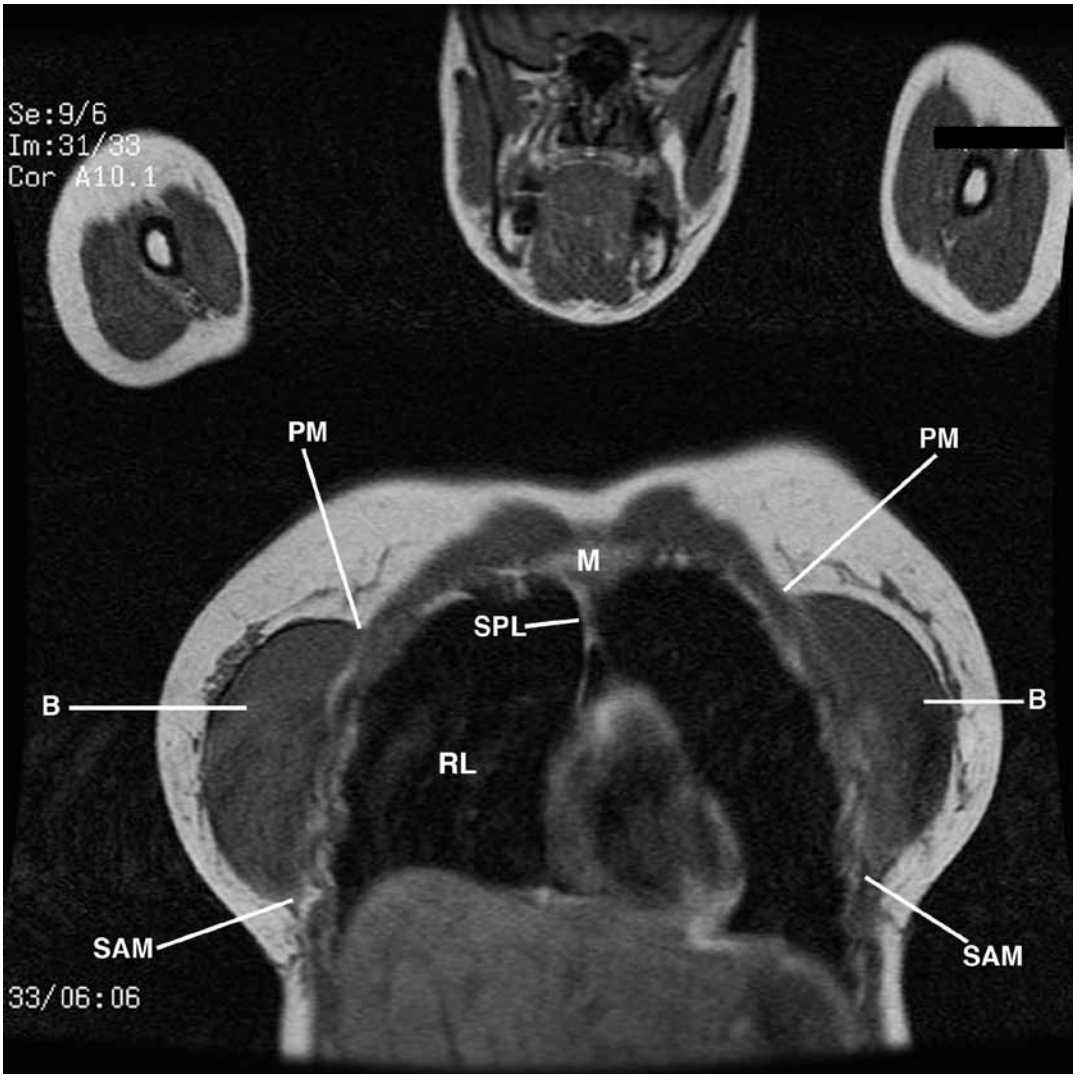

Observe the right lateral displaced super sternopericardial ligament (SPL) attaching to the manubrium (M).
RL indicates right lung.

indicate that some form of esophageal obstruction would be displayed by bilateral brachial plexus MRI, MRA, or MRV imaging. Of course, this was the case, as described above. Therefore, TOS, migraine, carpal tunnel syndrome, and piriformis sinus syndrome are clinical diagnoses. They have a pathological cause, and one must look at the decrease in blood flow as the contributing cause.[2] This Radiology Rounds presentation demonstrates the importance of having the clinical history and knowledge of anatomy and pathophysiology in making an accurate diagnosis.

ACKNOWLEDGMENT

Thanks to Steven Do at UCLA Radiology Media Center.

REFERENCES

1. Collins JD, Saxton E, Miller TQ, Ahn S, Gelabert H, Carnes A. Scheuermann's Disease As A Model Displaying the Mechanism of Venous Obstruction in Thoracic Outlet Syndrome and Migraine Patients: MRI and MRA. *J Natl Med Assoc*. 2003;4:298-306.

2. Collins JD. www.tosinfo.com. Accessed September 30, 2012.

3. Woodburne RT, Burkel WE. Essentials of Human Anatomy. 8th ed. New York, NY: Oxford University Press; 1988;18-216.

4. Collins JD, Shaver M, Disher A, Miller TQ. Compromising abnormalities of the brachial plexus as displayed by magnetic resonance imaging. *Clin Anat*. 1995;l8:1-16.

5. Saxton E, Collins JD, Miller TQ, Ahn S, Gelabert H, Carnes A. Right aortic arch, aberrant left subclavian artery and ruptured breast implants presenting with thoracic outlet syndrome (TOS) and migraine: MRI, MRA, MRV. *Faseb J*. 2009;23:474.5.

6.Atassoy E. Thoracic outlet compression syndrome. *Orthop Clin N Am*. 1996;27:265-303.

7. Lord JW, Rosati LM. Thoracic outlet syndromes. *Clinical Symposia Ciba Geigy*. 1971:1-32.

8. Sunderland S. Blood supply of the nerves to the upper limb in man. *Arch Neurol Psych*. 1945;53:91-115.

9. Batson OV. The function of the vertebral veins and their role in the spread of metastases. *Ann Surg*. 1940; 112:138.

10. Batson OV. The vertebral vein system. *Am J Roentgen*. 1957; 78:195-212.

11. Groen RJ, Grobbelaar M, Muller CJ, Van Solinge G, et al. Morphology of the Human Internal Vertebral Venous Plexus: A Cadaver Study After Latex Injection in the 21-25-Week Fetus. *Clin Anat*. 2005;18:397.

12. Clemente, CD. Anatomy, A Regional Atlas of The Human Body. 5th ed. Baltimore, MD: Lippincott Williams and Wilkins; 2007.

13. Collins JD. A Woman Post Scalenectomy and First-Rib Resection With Dilated Vertebral Venous Plexus and a Facial Rash. *J Natl Med Assoc*. 2012;104:306-310. ■